

Article

Effect of Polymer Adjuvant Type and Concentration on Atomization Characteristics of Nozzle

Peng Hu ¹, Ruirui Zhang ^{1,*}, Liping Chen ², Longlong Li ², Qing Tang ², Wenlong Yan ² and Jiajun Yang ^{1,2}

¹ School of Mechanical and Electrical Engineering, Xinjiang Agricultural University, Urumqi 830052, China; hp2469730431@163.com (P.H.); 17311715713@163.com (J.Y.)

² Research Center of Intelligent Equipment, Beijing Academy of Agricultural and Forestry Sciences, Beijing 100097, China; chenlp@nercita.org.cn (L.C.); lill@nercita.org.cn (L.L.); tangq@nercita.org.cn (Q.T.); 2222216001@stmail.ujs.edu.cn (W.Y.)

* Correspondence: zhangrr@nercita.org.cn; Tel.: +86-010-51503991

Abstract: (1) Background: Various types of adjuvants are added during application to enhance the spraying effect, but most adjuvant formulations are proprietary products, and their exact compositions have not been disclosed. (2) Methods: The spatial distributions of droplet sizes and velocities generated by the atomization of different polymer adjuvants were measured based on the phase Doppler interferometer (PDI) measurement method. The sub-area statistical method was used to quantitatively analyze the droplet characteristics at various points below the nozzle. (3) Results: The polymer (polyethylene oxide (PEO))/associative surfactant (sodium dodecyl sulfate (SDS)) can increase the droplet size and velocity of the solution after atomization by increasing the amount of the polymer/associative surfactant to reduce the equilibrium surface tension of the solution and increase the viscosity. Different concentrations of polymer/associative surfactant atomization produced larger droplet sizes and better uniformity than polymer/non-associative surfactant (polysorbate-20 (Tween20)). At the same position, the relationship between droplet velocities for the three adjuvant combinations was roughly as follows: PEO/SDS solution had the highest velocity, followed by PEO solution, and PEO/Tween20 solution had the lowest velocity. (4) Conclusions: The optimal of droplet size distribution can be achieved by adding appropriate amounts of associative surfactants to polymers.



Citation: Hu, P.; Zhang, R.; Chen, L.; Li, L.; Tang, Q.; Yan, W.; Yang, J. Effect of Polymer Adjuvant Type and Concentration on Atomization Characteristics of Nozzle. *Agriculture* **2024**, *14*, 404. <https://doi.org/10.3390/agriculture14030404>

Academic Editor: Dainius Steponavičius

Received: 25 January 2024
Revised: 27 February 2024
Accepted: 29 February 2024
Published: 1 March 2024



Copyright: © 2024 by the authors. Licensee MDPI, Basel, Switzerland. This article is an open access article distributed under the terms and conditions of the Creative Commons Attribution (CC BY) license (<https://creativecommons.org/licenses/by/4.0/>).

Keywords: polymer adjuvant; atomization; nozzle; PDI

1. Introduction

In crop production, pesticide spraying remains one of the common methods for preventing and controlling diseases, pests, and weeds. The nozzle is a crucial component during the pesticide application process. Its function is to atomize the pesticide into droplets and then, under the influence of external forces, deliver the liquid to the target crops. The size distribution and velocity distribution of the droplets directly impact the movement of droplets during transport, influencing the drift and deposition rate, thereby further affecting the utilization efficiency of pesticides and the effectiveness of pest control. Small droplets exhibit favorable deposition and coverage effects but are susceptible to evaporation and drift, which can affect their application efficacy. Oversized droplets can result in the loss of liquid on crop leaves to the soil, causing soil pollution and reducing pesticide utilization efficiency. Droplet velocity also affects pesticide utilization. Droplets with extremely low velocities cannot reach the target, while those with excessively high velocities are prone to bouncing back [1–4].

To improve the quality of pesticide application and pesticide utilization efficiency in crop production, various types of adjuvants are usually added. The addition of specialized adjuvants to aerial plant protection agents has many advantages. For example, it can increase

the settling rate of droplets, increase the ratio of fine droplets to reduce drift, decrease evaporation of the liquid in high-temperature and windy conditions, enhance the adhesion rate of the liquid on crop surfaces, and improve the spreading and penetration of the liquid on the crop surface [5–7]. Pesticide adjuvants can be classified based on their usage in pesticides, functions, surfactant properties, structural types, molecular sizes, etc. [8–12].

In recent years, scholars both domestically and internationally have conducted relevant research on the spatial distribution characteristics of droplet size and velocity during the atomization of solutions with different types of adjuvants. Zhang et al. [13] have compared and analyzed the differences in median droplet volume and relative span of droplet distribution for IDK120-025 and LU120-015 nozzles spraying solutions with different concentrations of typical synergist adjuvant, as well as yield-enhancing adjuvant and urea, using a laser particle size analyzer. Li et al. [14,15] have explored the impact of different adjuvants and pressures on the spatial distribution of droplet size and droplet velocity in different atomization areas of various nozzles using a phase Doppler interferometer (PDI). Zhang et al. [16] have utilized a phase Doppler particle analyzer (PDPA) to measure the droplet movement velocity within the spray fan of a LU120-03 fan atomizing nozzle and determined the velocity distribution of droplets in the spray area. Li et al. [17] have used a PDPA to measure the atomization characteristics of a fan nozzle under different spraying parameters, establishing models for droplet size and velocity. Chen et al. [18] have employed a laser particle size analyzer to measure droplet size information in the atomization field of a small-angle fan nozzle. They calculated the uniformity of droplets under different parameters and analyzed the weight of factors affecting droplet uniformity under various conditions. Vallet et al. [19] have studied the impact of adjuvants on atomization characteristics and the atomization characteristics of different nozzles under different pressures. Thompson et al. [20], in exploring the atomization principles of planar fan nozzles and hollow-cone misting nozzles, applied fluid dynamic analysis, finding that droplets at low speeds increase with increasing misting pressure, while the atomization liquid film of viscous fluids stretches and thins with increasing misting pressure. It breaks into fine droplets when the liquid's velocity exceeds the critical speed of film rupture. Roudini et al. [21] have used high-speed cameras combined with particle tracking and phase Doppler anemometry (PDA) to study the droplet size distribution curves of different liquids in the axial and radial directions. The results showed that equilibrium surface tension and viscosity influenced the entire atomization process and had a significant impact on droplet size distribution. Tang et al. [22] have used PDI to measure the droplet size and velocity distribution at different lateral sampling points below the nozzle at a specific pressure. The researchers mentioned above employed different measurement methods to study the atomization characteristics of nozzles under various conditions, and the adjuvants investigated were commercial adjuvants, lacking exploration into their specific compositions.

It is well known that surfactants and polymers are usually present in sprayed liquids, and their role is mainly to enhance the spray effect and reduce drift and liquid bounce. Surfactant–polymer interactions can be described as both associative and non-associative. Changes in solution viscosity and surface properties induced by the adjuvant are critical in determining spray performance; however, little is known about how these changes affect spray performance in terms of droplet size and velocity distribution. Therefore, it is necessary to investigate the relative effects of polymer/associative surfactant versus polymer/non-associative surfactant systems in improving droplet size and velocity. Polyethylene oxide (PEO) is mainly used in pesticide spray liquids as a thickening agent, adhesion agent, and humectant, which helps to improve liquid viscosity, make the spray uniform and less prone to loss, increase the adhesion of pesticide spray liquids, and increase pesticide adherence on the surface of plants. Sodium dodecyl sulfate (SDS) is mainly used as a humidifier, emulsifier, and penetrant in pesticide spray liquid, which helps to improve the surface tension of pesticide spray liquid, improve the dispersion and stability of pesticides in water, and increase the absorption and effect of pesticides in the body of plants. PEO and SDS can form flexible high-molecular-weight polymer–anionic surfactant

complexes, and their structure has been thoroughly studied [23,24]. As most formulations of agricultural chemicals are proprietary products with undisclosed exact compositions, PEO, SDS, and polysorbate-20 (Tween20) were chosen as model systems for this study. This study utilized the PDI measurement method to measure the spatial distribution of droplet size and the velocity produced by different polymer adjuvants. A sub-area statistics method was employed to statistically analyze the droplet characteristics at various points beneath the nozzle. Quantitative analysis was conducted on the spatial distribution of droplet size and the velocity produced by different polymer additive solutions. This clarifies the influence patterns of different polymer adjuvant components on nozzle atomization characteristics, providing a reference for the development of new adjuvant compositions.

2. Materials and Methods

2.1. Nozzle and Solution Selection

Fan nozzles can generate a fan-shaped atomization area with a substantial atomization volume that maintains central symmetry, ensuring a uniform distribution of the spray volume [25]. Therefore, this study selected the experimental nozzle LU120-03 from Lechler, Germany. The spray angle was 120° , the recommended spray pressure range was 150–500 kPa, the corresponding flow rate range was 0.84–1.53 L/min, and the nozzle structure is shown in Figure 1. The experimental adjuvants included three polymers: PEO (Guangzhou Lihou Trading Co. Ltd.; Guangzhou, China), Tween20 (Guangzhou Saiguo Biotech Co. Ltd.; Guangzhou, China), and SDS (Fuzhou Feijin Biotech Co. Ltd.; Fuzhou, China). The specific types and critical micelle concentrations are shown in Table 1.

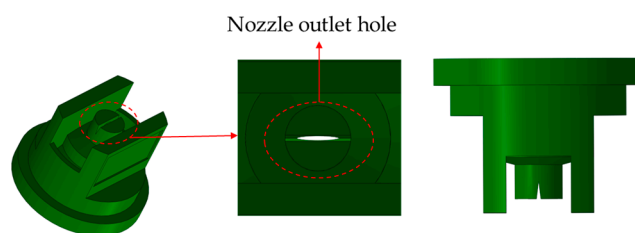


Figure 1. LU120-03 nozzle structure.

Table 1. Detailed list of adjuvants.

Type of Adjuvant	Name	Critical Micelle Concentration (CMC)
Polymer	PEO	0.075 wt%
Nonionic surfactants	Tween20	0.06 mM
Anionic surfactants	SDS	7–10 mM

2.2. Basic Theory

Fan pressure nozzle atomization is a process where a liquid medium, under the influence of external forces, is forced through the nozzle and sprayed into the surrounding air to form a liquid film. The liquid film experiences a velocity difference, leading to mutual collisions that generate a shearing effect, forming liquid bands. Eventually, these liquid bands fragment into droplets. This droplet fragmentation is influenced by various factors, including the equilibrium surface tension of the liquid, viscous forces, and interactions with the surrounding air. The equilibrium surface tension and viscous forces of the liquid inhibit the destabilization and deformation of the liquid film surface. A liquid film breaks into droplets only when the external force exceeds the force required to maintain the cohesive state of the liquid [26].

Spray droplet size is typically represented by characteristic points on the droplet diameter distribution curve, referred to as the characteristic diameters of the droplets. These diameters include $D_{v0.1}$, $D_{v0.5}$, $D_{v0.9}$, etc. $D_{v0.5}$ represents the droplet volume median diameter, which signifies the diameter at which 50% of the total volume of droplets is accumulated in the droplet size distribution. $D_{v0.5}$ is also known as the volume median

diameter (VMD). Because the results of this study are mainly used as a reference for agricultural spraying applications, the droplet volume median diameter is used as the average size of the droplets, which is the most commonly used presentation of droplet size in the analysis of spraying characteristics in the process of pesticide application operations. The droplet volume median diameter is calculated by the following formula:

$$VMD = \left(\frac{\sum d_i^3 N_i}{\sum N_i} \right)^{1/3}, \quad (1)$$

where d_i represents the diameter of the i th droplet, μm ; N_i represents the number of droplets with a diameter of d_i .

For droplets in the atomization area, the average droplet speed was chosen, and the definition of average droplet speed is expressed as follows:

$$v = \frac{\int_{v_{min}}^{v_{max}} V dn}{\int_{v_{min}}^{v_{max}} dn}, \quad (2)$$

In the formula, v represents the average droplet speed at the measurement point, m/s ; v_{max} represents the maximum droplet speed, m/s ; v_{min} represents the minimum droplet speed, m/s ; V represents the droplet speed, m/s .

At present, the relative span (RS) of droplet size distribution is commonly employed to analyze and assess the uniformity of spray from nozzles. The RS value is calculated using a formula.

$$RS = \frac{D_{v0.9} - D_{v0.1}}{D_{v0.5}}, \quad (3)$$

In this study, the average droplet speed (v) serves as the parameter for the spatial distribution of droplet speeds, while $D_{v0.5}$ is used as the parameter for the spatial distribution of droplet sizes.

2.3. Measurement Platform Construction

The nozzle droplet parameter measurement platform is shown in Figure 2. This platform consists of a spray control system, a three-dimensional movement control system, and a droplet measurement device. The spray control system is designed independently by the National Agricultural Intelligent Equipment Technology Research Center. The system includes a ton barrel, electric agitator, smart electric diaphragm pump, pressure stabilization tank, pressure gauge, flowmeter, and nozzles. The smart electric diaphragm pump is adjusted to accurately control the spray pressure in real time. The three-dimensional movement control system moves the PDI, fixed on the transport device, to the measurement points to measure the droplet atomization characteristics. It is controlled by three Siemens Simodrive Posmo A motors in the XYZ directions, and the motors are controlled by a Siemens Programmable Logic Controller (PLC) with a movement accuracy of 0.1 mm. The droplet measurement device uses a PDI, model PDI-300MD, produced by Artium company in Sunnyvale, CA, USA. The PDI includes an optical emitter, optical receiver, advanced signal analyzer (ASA), data management computer, and the Automated Instrument Management System 2.3.0.1 (AIMS) software package. The modulated optical transmitter emits a green laser beam with a wavelength of 532 nm, which is split into two beams of equal intensity by a laser beam splitter, and the two laser beams are passed through a lens to make them intersect and focus together to measure the droplet information. The laser intersection point needs to be manually focused on the plane of the liquid film formed by the atomization of the fan nozzle before measurement. The eyepiece on the optical receiver is adjusted by observation to adjust the angle between the optical receiver and the optical transmitter so that a clearly visible green beam is present in the interference slit. The PDI measures droplet sizes from 0.3 to 7000 μm (spherical), with a measurement accuracy of

± 0.5 and a resolution of $\pm 0.5 \mu\text{m}$, and velocity measurements in the range of -600 to 1000 m/s . The speed accuracy is $\pm 0.1\%$.

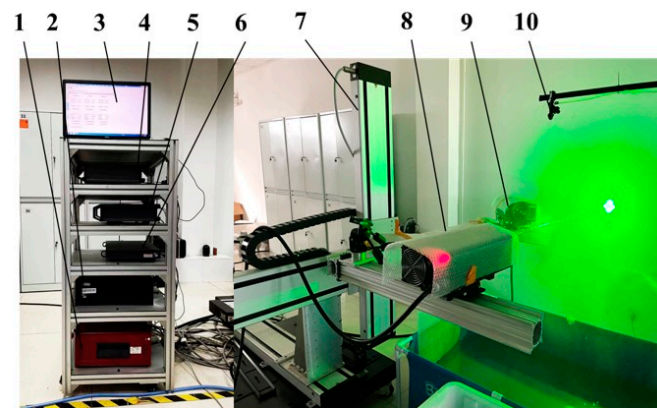


Figure 2. Droplet parameter measurement platform. 1. Power supply 2. Data management computer 3. AIMS 2.3.0.1 system software 4. Signal processor 1 channel 5. Signal processor 2 channel 6. Signal processor 3 channel 7. 3-axis positioning and moving system 8. Optical transmitter 9. Optical receiver 10. Nozzle.

2.4. Experimental Design and Methodology

The experiments were conducted in a controlled environment to minimize the influence of external factors. The experiment was conducted under the enclosed space without wind and light, and the temperature was maintained at $20\text{--}22 \text{ }^\circ\text{C}$ with a humidity range of $20\text{--}50\%$. The controlled environment ensured that droplet evaporation could be neglected. This study focused on a basic model of a fan spray area for agricultural spraying applications. Considering the effect of gravity, the nozzle was positioned vertically downward. A spatial right-angle coordinate system was established with the nozzle outlet center as the origin. The x -, y -axis-, and z -axes represent the long, short, and spray axes of the spray cross section, respectively. The droplets sprayed from the fan spray nozzle are approximately distributed in a plane, so the measurement is mainly focused on the droplet characteristic parameters in the X, Z plane.

The pressure gradients set for this study were $150, 200, 250, 300,$ and 350 kPa , which cover the commonly used operating pressure setting range. Because the atomization area of the standard fan nozzle is centrosymmetric, the experimental program set the measurement sub-areas to cover half of the atomization area and the measurements were made at heights of $0.1, 0.2, 0.3, 0.4, 0.5,$ and 0.6 m , measured vertically down from the nozzle [27,28]. Each height level, originating from the spray axis, had measurement zones spaced 0.05 m apart along the horizontal x -axis, extending to the edge of the spray area. The average values of atomization parameters within each measurement sub-area were taken as the actual values for the corresponding sub-area, as shown in Figure 3. When measuring to the edge of the spray, the data obtained are not of research value because the PDI does not capture enough data. Therefore, the measurement data rate was set to stop measuring data values for this height class when the measurement data rate was less than 2 pcs/s , and the previous sub-area was the last sub-area of this height class.

To ensure the accuracy of measurement data, the nozzle was set at a fixed height, and the AIMS system software was used to set the position of each data sampling point. The PDI was moved for sampling using the PLC-controlled three-dimensional positioning system. Each measurement point was repeated three times, with each measurement lasting for 30 s . The average of the three repeated data measurements was taken as the droplet size and velocity for that measurement point.

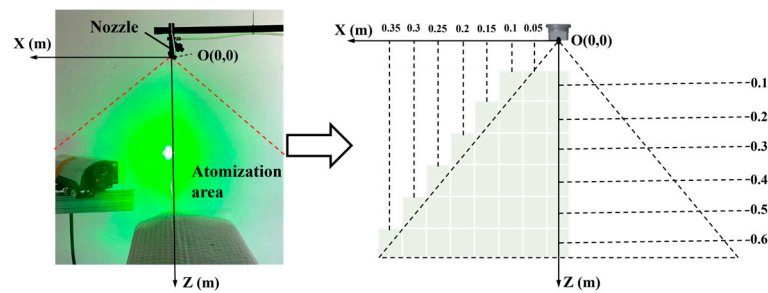


Figure 3. Distribution schematic of fan nozzle spray area measurement sub-areas.

For all the solutions, the PEO concentration was maintained at a constant 0.075 wt%, which is semi-dilute and similar to the rate of polymer use (0.02–0.05%) contained in agricultural spray mixtures. Four concentrations of the two systems' surfactants were set at 0.5 CMC, 1 CMC, 2 CMC, and 4 CMC. The mass concentrations corresponding to the different combinations of adjuvants are denoted by the symbol ρ_n in kg/m^3 . Further, 0.075 wt% of PEO solution had a mass concentration of $0.75 \text{ kg}/\text{m}^3$, 1CMC of PEO/SDS solution had a mass concentration of $1.907 \text{ kg}/\text{m}^3$, and 1CMC of PEO/Tween20 solution had a mass concentration of $0.06 \text{ kg}/\text{m}^3$. This was achieved by stirring the PEO solution with an electric stirrer, followed by the addition of a suitable amount of SDS powder, and thorough stirring for 24 h to prepare the PEO/SDS mixed solution. The PEO/Tween20 mixed solution was prepared using the same procedure. During the experiment, the mixed solutions were prepared according to specified amounts and tap water was sprayed as a control group before conducting each set of experiments. Equilibrium surface tension and viscosity measurements were performed on solutions with different concentrations of each adjuvant combination. When using PDI to measure the droplet parameters, the size of the spray flow rate was measured in real time, and the results showed that the spray flow rate increased with the increase in the spray pressure; additionally, a linear relationship with a strong correlation between the spray pressure and the flow rate was found by fitting. Different adjuvant solutions had the same flow rate under the same spray pressure condition. Therefore, only the spray pressure was chosen as the independent variable in the following discussion.

3. Results

3.1. Analysis of Physical Properties of Polymer Adjuvants

The equilibrium surface tension and viscosity results of pure the PEO, PEO/SDS, and PEO/Tween20 solutions measured by using an equilibrium surface tension meter and viscometer are shown in Figure 4. Surfactants reduce the equilibrium surface tension of water by adsorbing at the liquid–air interface. Comparing the data in the graph, the equilibrium surface tension of the PEO/SDS solution gradually decreased with increasing SDS content, reaching a reduction of 58.9% relative to water when the solution concentration reached 4CMC. The addition of 0.5CMC SDS to the PEO solution resulted in a slight increase in viscosity, reaching its maximum at 2CMC, and further addition of SDS led to a slight decrease in viscosity. In the case of adding anionic surfactant SDS to the high-molecular-weight polymer PEO, at the initial stage, individual SDS molecules associated with PEO chains, forming aggregates on the main chain and causing slight expansion of the chain due to electrostatic repulsion between the negatively charged groups of SDS molecules. When the concentration reached 2CMC, the PEO helix was saturated with SDS micelles, reaching the maximum level of complexation, and the solution viscosity peaked [29]. Conversely, the addition of a certain amount of Tween20 to PEO solution resulted in no significant changes in equilibrium surface tension and viscosity values, as shown for the pure PEO solution. This may be because the concentration of Tween20 added to the PEO solution is in the range of 0.5 to 4CMC, which is too small to significantly reduce the equilibrium surface tension and viscosity values. As the concentration of the PEO/SDS and the PEO/Tween20 solutions increased, the difference in equilibrium surface tension and viscosity between

the two solutions may have led to differences in the characteristics of atomization to form droplets.

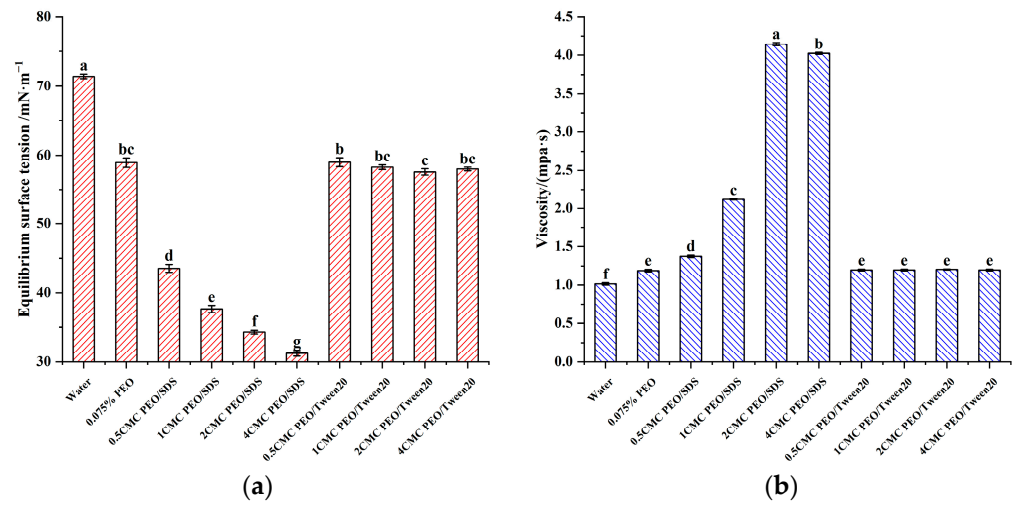


Figure 4. Viscosity and equilibrium surface tension distribution of solutions with different concentrations of adjuvants. (a) Viscosity distribution graph. (b) Equilibrium surface tension distribution graph. (Note: The graphs a–g are arranged according to the size of all means, with a representing the largest mean, and where there is a letter with the same labeling, the difference is not significant, and where there is a letter with a different labeling, the difference is significant.)

3.2. Spatial Distribution of Droplet Size

3.2.1. Characterization of Droplet Size Distribution in Vertical Direction

To obtain average droplet sizes on the Z-axis cross-section, the sizes in different sub-areas on the Z-axis were weighted and averaged by using the number of droplets. At a pressure of 250 kPa, the droplet size distribution below the LU-120-03 nozzle in the vertical direction for different adjuvants combinations is shown in Figure 5a. There was a 26.24% increase in droplet size in the Z-axis cross-section with the addition of 0.075 wt% PEO adjuvant alone as compared to water. The addition of small amounts of polymer molecules to sprayed liquids has been shown to result in the formation of larger droplets [30,31]. The main reason for this is that the addition of PEO increases the viscoelasticity of the solution and forms a film between the water and air, reducing the dynamic surface tension, which means that there is less of an energy barrier to droplet formation, resulting in an increase in the droplet sizes formed by the rupture of the liquid film. In addition, PEO can change the flow properties of water, making it easier for droplets to merge during formation and movement, leading to an increase in droplet size. When Tween20 was added to the PEO solution, the droplet size was significantly reduced and the size was close to that of water; furthermore, increasing the concentration of Tween20 had a small effect on the droplet size. The PEO/Tween20 mixtures at different CMCs have equilibrium surface tensions and viscosities relatively close to water. In addition, the dynamic surface tension of the mixtures in the first milliseconds of the atomization should be much closer to the water equilibrium surface tension, so the experimental results are simply the expected ones. For the PEO/SDS combination, as the SDS concentration increases, the equilibrium surface tension of the polymer decreases, viscosity increases, and droplet size increases accordingly. When the PEO/SDS concentration reaches 4CMC, the droplet size increases by about 47% compared to water, demonstrating a significant increase in droplet size. Thus, for polymer/associative surfactant combinations, it is possible to increase the droplet size by increasing the amount of the associative surfactant.

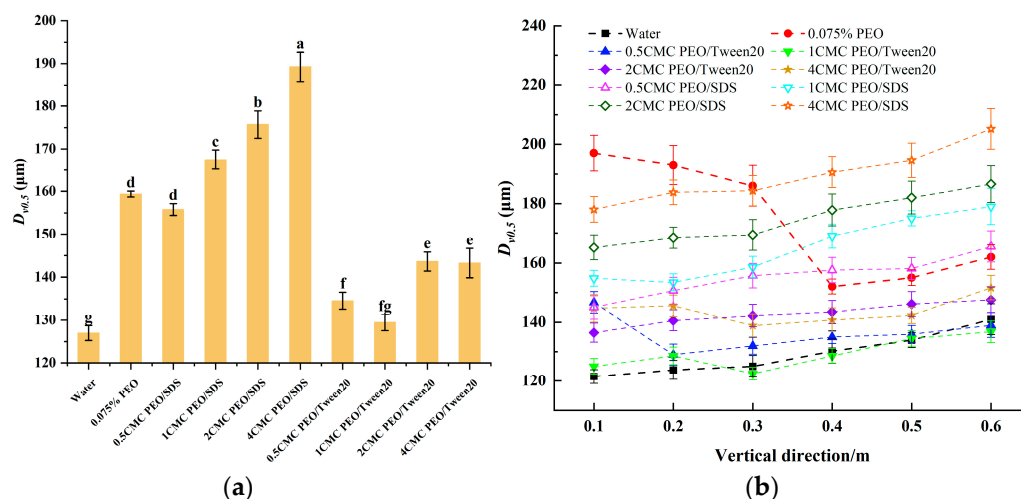


Figure 5. Droplet size distribution in vertical direction at 250 kPa pressure. (a) z-axis cross-section. (b) Vertical direction. (Note: The graphs a–g are arranged according to the size of all means, with a representing the largest mean, and where there is a letter with the same labeling, the difference is not significant, and where there is a letter with a different labeling, the difference is significant.).

At a pressure of 250 kPa, the droplet size distributions in the vertical direction for different adjuvant combinations is shown in Figure 5b. The droplet size distribution of water exhibits a gradually increasing trend. The droplet size in the pure PEO solution is initially the largest during atomization, with a gradual decrease along the vertical direction. As the viscosity of the PEO solution increases, the atomization produces an increase in the length of the liquid film breakage, the liquid film breakage of the droplets formed by the viscous force and the role of air resistance, and the formation of secondary rupture of the droplet movement process, making the droplet size gradually decrease. At a distance of 0.4 m below the nozzle, a change in droplet size occurs, with the droplet size gradually increasing, and collisions and coalescence between large and small droplets occurring. The droplet sizes in the PEO/Tween20 solutions at different concentrations are lower than those in the pure PEO solution, and the droplet sizes are closer to those in the water solution. The droplet sizes in the PEO/SDS solutions at different concentrations are larger than those in the PEO/Tween20 solutions. The droplet sizes increase along the vertical direction, with smaller droplet sizes than pure PEO in the early stages of atomization. After reaching 0.4 m below the nozzle, the PEO/SDS solution has the largest droplet sizes, exhibiting an overall uniform droplet size distribution. Moreover, higher SDS concentrations result in larger droplet sizes.

3.2.2. Characterization of Droplet Size Distribution in Horizontal Direction

The farthest end of the measurement area below the nozzle is 0.6 m, which is the closest distance to the crop canopy, making the droplet size distribution characteristics here more valuable for reference. Therefore, the positions at $z = 0.6$ m below the nozzle under different pressure conditions were selected for the analysis of droplet sizes, as shown in Figure 6. The droplet size of the different atomized adjuvants decreased with the increase in spray pressure. The droplet sizes atomized by the PEO solution under different spray pressure conditions were larger than those of the PEO/Tween20 solution. At pressures of 150 kPa, the droplet sizes of the PEO/SDS solutions with concentrations of 1, 2, and 4 CMC were larger than those of the pure PEO solutions in the x -axis interval from 0 to 0.25 m. The pure PEO solution has the largest droplet size, indicating an increase in droplet size and improved uniformity with the addition of SDS to the PEO solution. At pressures of 250 kPa, the droplet size of the PEO/SDS solutions with concentrations of 1, 2, and 4 CMC in the range of 0 to 0.35 m in the x axis were larger than that of the pure PEO solution. At a pressure of 350 kPa, the droplet size of the 4CMC PEO/SDS solution was the largest. This

is when the equilibrium surface tension is minimized and the liquid film ejected from the nozzle under spray pressure has the shortest break-up length, breaking up to form a large number of large droplets. This is the ideal result for spraying, as it may lead to less drift and better penetration.

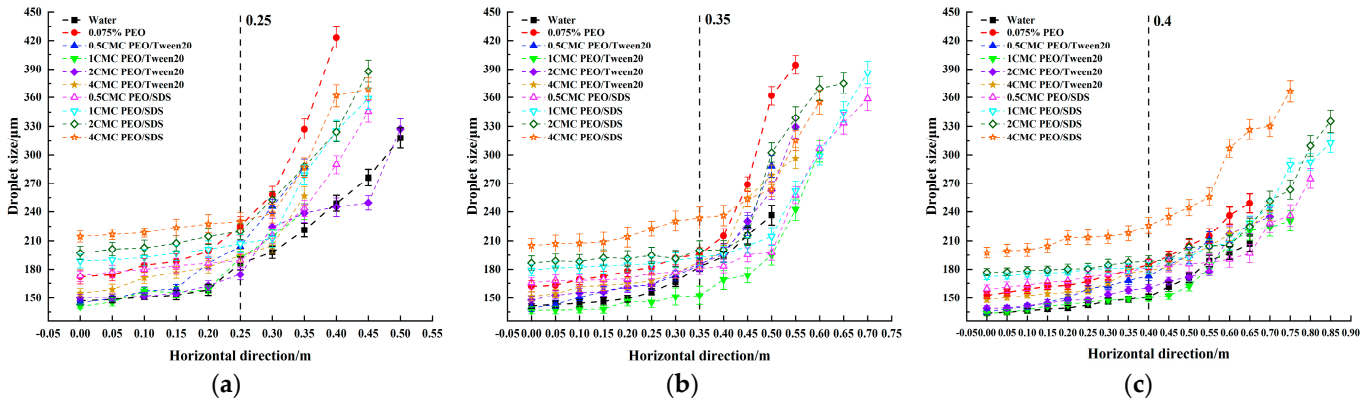


Figure 6. Droplet size distribution at $z = 0.6$ m under different spray pressures. (a) 150 kPa; (b) 250 kPa; (c) 350 kPa.

An analysis of droplet sizes under different concentrations of adjuvants at a spray pressure of 250 kPa was conducted. From Figure 7, it can be observed that, at the same horizontal plane below the nozzle, droplet sizes of solutions with different adjuvant concentrations gradually increase along the horizontal direction, with the maximum size at the periphery. When the liquid is sprayed to form a liquid film, the edge of the liquid film becomes unstable due to the effect of the equilibrium surface tension. This instability will lead to fluctuations and distortions at the edge of the liquid film, which will eventually lead to the rupture of the liquid film into droplets. The rupture of the edge of the liquid film is subject to the constraints of the viscous force, which is the main reason for the large droplet size formed by the crushing of the edge of the liquid film. The evaporation and collision of droplets in the spray area play a crucial role in influencing droplet sizes. Evaporation reduces the size of large droplets, while collision between droplets can lead to the coalescence into larger droplets; additionally, the farther from the nozzle, the more numerous the large droplets are. Both factors contribute to a reduction in the number of droplets, changes in the average droplet diameter, and the redistribution of sizes. Since the center of the spray area is farthest from the spray edge, the probability of droplet collision increases at the central position, leading to the occurrence of secondary atomization. The formula for fluid aerodynamic resistance is as follows:

$$F_D = C_D \frac{\rho_g |v - v_p| (v - v_p)}{2} \frac{\pi d_p^2}{4}, \quad (4)$$

In the formula: F_D represents the air resistance acting on droplets, C_D is the air resistance coefficient, ρ_g is the air density, v is the air velocity, v_p is the droplet velocity, and d_p is the droplet diameter. It can be observed that large droplets experience greater aerodynamic forces than small droplets, resulting in smaller total acceleration for large droplets. Droplets decelerate due to air resistance, and smaller droplets experience faster deceleration due to the blocking effect of air. Large droplets possess greater initial kinetic energy, making their trajectories less susceptible to influences.

Under the same pressure conditions, the droplet sizes in solutions with different adjuvants were larger than those in the water solutions. The droplets produced by the pure PEO solution had the largest sizes in the range of 0.1 to 0.3 m below the nozzle, and the droplets produced in the range of 0.4 to 0.6 m were largest near the edge of the spray area. The droplet sizes of the PEO/SDS adjuvant solution within the range of 0 to 0.25 near the Z-axis were larger than those of the PEO/Tween20 adjuvant solution. The spray range of

the PEO/SDS adjuvant solution was increased compared to the pure water and pure PEO solutions. Differences in the tensile properties of PEO solutions because of the increase in SDS addition may produce significant differences in the flow behavior of these fluids within the nozzle prior to departure and rupture [32]. The droplet sizes produced by the PEO/SDS solution gradually increased with the increase in solution concentration, while the addition of Tween20 to the PEO solution resulted in a reduction in droplet sizes during atomization. Under steady-state conditions with no external forces applied, PEO molecular chains will remain coiled in the absence of or in low concentration of SDS in the PEO solution, while at higher SDS concentrations the resting state conformation of the PEO molecular chains is more extended [33,34]. The reason for this change in steady-state conformation is the increase in surfactant aggregates (which ultimately form micelle-like structures) throughout the length of the PEO molecular chain with increasing SDS concentration [35]. This increase in surfactant aggregates reduces the number of intra-chain interactions because of the presence of negatively charged SDS chains and aggregates. Such a property allows for the PEO/SDS solution to produce a larger spray angle during spray nozzle atomization, which also increases the area of the spray nozzle atomization operation.

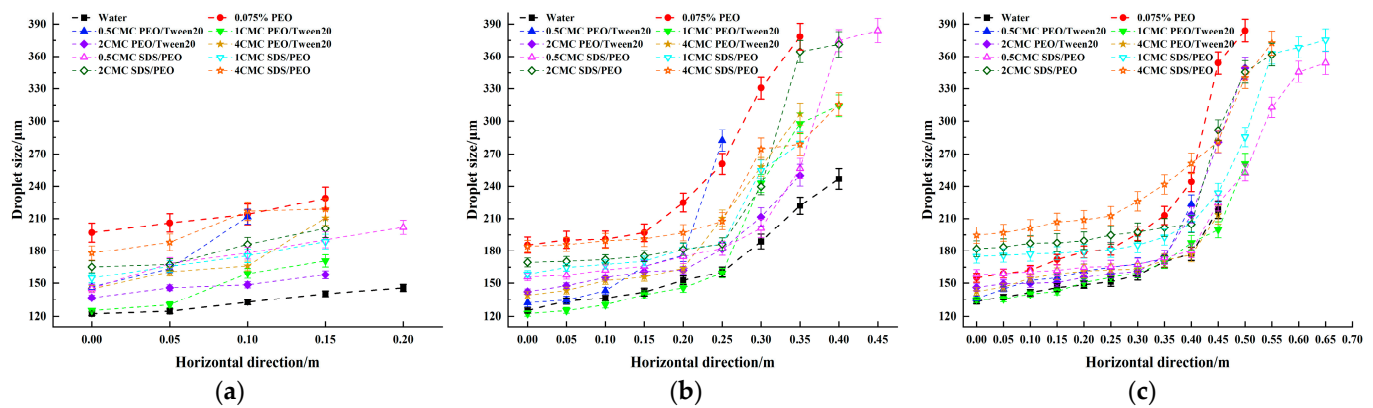


Figure 7. Droplet size distribution at spray pressure of 250 kPa. (a) $z = 0.1$ m; (b) $z = 0.3$ m; (c) $z = 0.5$ m.

3.2.3. Spray Pattern Droplet Size Spatial Distribution Uniformity Analysis

Figure 8 illustrates the impact on the uniformity of droplet size distribution at a distance of 0.6 m below the nozzle with varying spray pressures and horizontal distances. The RS of the particle size distribution transforms droplet sizes into a dimensionless number, representing the uniformity of droplet sizes. A value closer to zero indicates more uniform droplet sizes. The ideal performance of a nozzle is to generate the minimum RS within a certain range [36]. From Figure 8, it can be observed that, in terms of droplet size uniformity, under the same pressure conditions, the RS values gradually decrease along the x -axis direction, indicating an increase in droplet size distribution uniformity. Closer to the edge of the spray area, the span of droplet size distribution becomes smaller, resulting in better uniformity in droplet sizes near the spray area's edge. With increasing pressure, the overall RS of the spray area gradually increases, indicating a decrease in overall uniformity. At a pressure of 150 kPa, the overall uniformity of the spray area is the best, likely due to the largest droplet sizes in the atomization field, making the droplets less prone to collisions and deviations. The RS of droplet sizes in the atomization of PEO/SDS solution is the smallest, indicating the most uniform droplet size distribution in the spray area. PEO and SDS interact significantly and form polymers, which leads to an increase in the viscosity of the solution and a small number of small droplets that are bound by viscous forces during solution atomization. As a result, the uniformity of droplet size distribution is better compared to the PEO solution and the PEO/Tween20 solution, which is the key to improving the application effect. Since there is no interaction between Tween20 molecular chains and PEO molecular chains, the RS of the droplet sizes in solution is closer to that of

the pure PEO solution, and the RS of the droplet sizes is larger than that of water. This is detrimental to the effectiveness of the application.

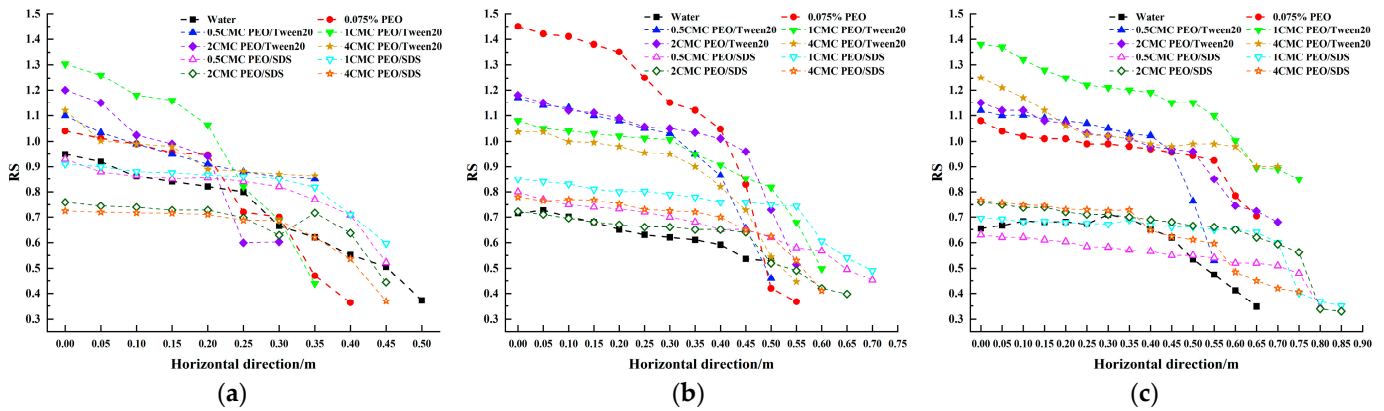


Figure 8. RS distribution of droplet size at different spray pressures. (a) 150 kPa; (b) 250 kPa; (c) 350 kPa.

3.3. Spatial Distribution of Droplet Velocity

An analysis of droplet velocities was conducted at a distance of 0.6 m below the nozzle, and the droplet velocity distribution at $z = 0.6$ m under different pressures is shown in Figure 9. The solid lines represent the fitted relationships between droplet velocity and the numerical x value on the x -axis. Under different pressure conditions, the droplet velocities of the various adjuvants gradually decrease along the horizontal direction, and at the same position, the droplet velocity is proportional to the pressure. The droplet velocity in the atomization of the PEO/SDS solution is significantly higher compared to the pure PEO solution, while the droplet velocity in the atomization of the PEO/Tween20 solution tends to decrease compared to water. The velocity of droplet motion is influenced by the difference between two interacting forces: the initial momentum of the liquid jet and the air resistance of the surrounding gas. The initial velocity of the liquid is high, but as the spray area moves and the number of atomized droplets increases, along with the increase in total surface area, the kinetic energy of the liquid gradually weakens due to friction with the environment. When the kinetic energy of the droplets is finally depleted, the droplets move with the motion of the surrounding gas or fall under the influence of gravity. The greater the injection pressure, the greater the initial sheet velocity and, consequently, the higher the velocity of the droplets. The droplet velocities for different adjuvant combinations were fitted with a quadratic polynomial function based on the numerical values on the x -axis, resulting in velocity models with R^2 values exceeding 0.9, indicating high accuracy. The fitted model is shown in Equation (5), and the fitting parameters and statistics for the model at a pressure of 250 kPa are presented in Table 2.

$$v = A_2x^2 + A_1x + A, \tag{5}$$

The distribution of the droplet velocities of the different adjuvant combination solutions in the vertical direction below the LU-120-03 nozzle at a spray pressure of 250 kPa was obtained by weighted average processing, as shown in Figure 10. The droplet velocity increased significantly with the addition of SDS to the PEO solution, with the greatest increase in droplet velocity relative to water being 27.9% at a concentration of 0.5 CMC. The change in droplet velocity with respect to water was not significant with the addition of 1 CMC SDS, and the droplet velocity gradually increased with the increase in SDS content. From the previous analysis, it can be seen that the droplet size formed by the atomization of the PEO/SDS solution increased significantly compared with PEO, which caused the droplets formed by atomization to have a larger initial kinetic energy and the speed of the droplets in the process of movement by the influence of air resistance decayed more slowly. As a result, the droplet velocity was greater under the same conditions. The regularity

presented by the addition of Tween20 to PEO is not significant enough, and more solutions with different concentration gradients may be needed for further investigation. At a concentration of 1CMC, the droplet velocity increased by 13.5% relative to water. Larger droplet velocities are needed in application because they increase the penetration of the solution, increase the application effect, and reduce the drifting phenomenon of the solution. Polymer/associative surfactant types were prioritized in the adjuvant selection process.

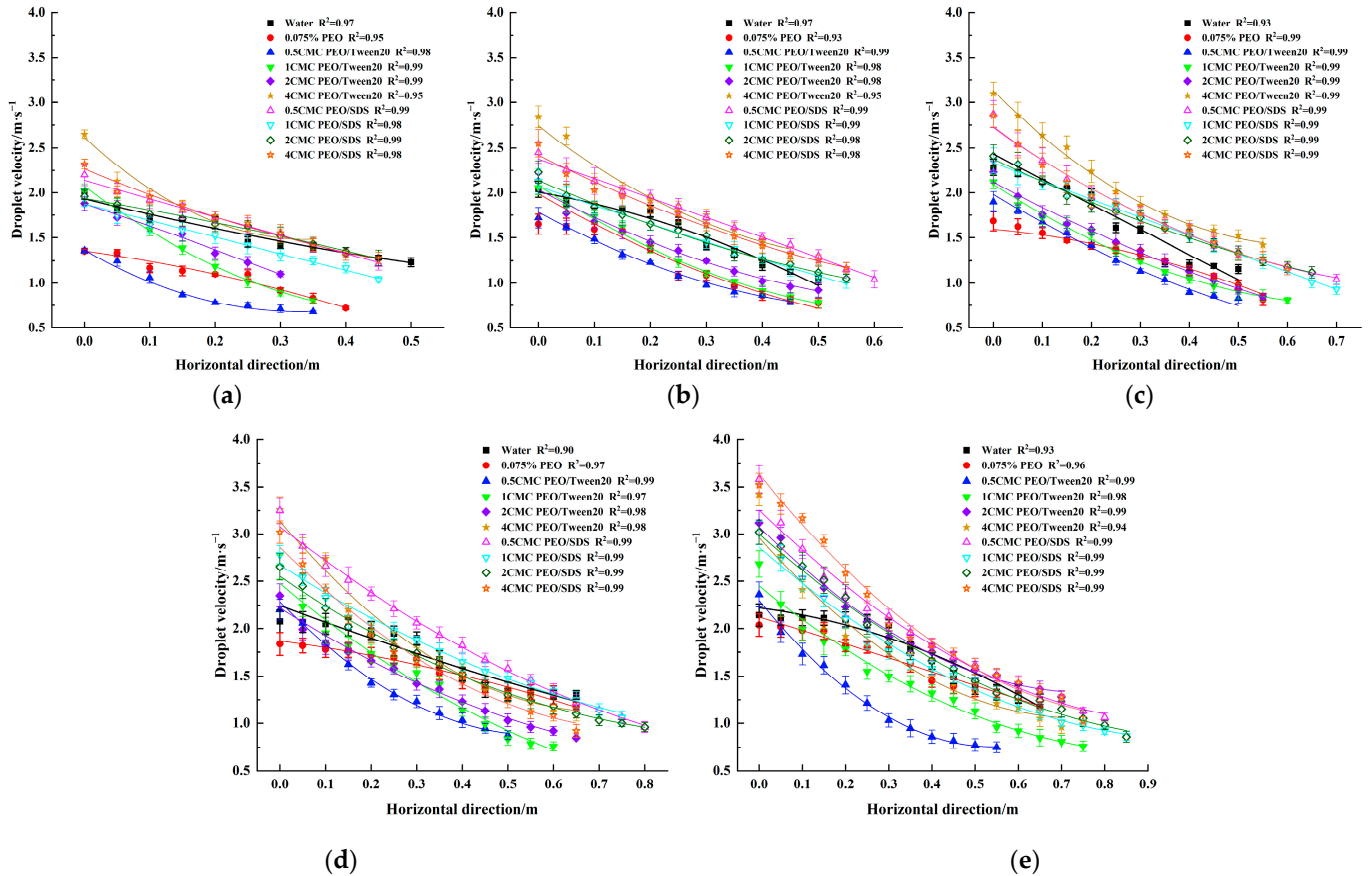


Figure 9. Distribution of droplet velocity at Z = 0.6 m under different pressures. (a) 150 kPa; (b) 200 kPa; (c) 250 kPa; (d) 300 kPa; (e) 350 kPa.

Table 2. Fitting parameters and statistics of the model at of 250 kPa pressure.

Droplet Velocity/m · s ⁻¹	Type of Adjuvant	A	A ₁	A ₂	R ²
v	Water	2.37	−2.85	0.40	0.93
	PEO	1.66	−0.85	−1.10	0.99
	0.5CMC PEO/Tween20	1.94	−3.09	1.55	0.99
	1CMC PEO/Tween20	2.09	−3.48	2.24	0.99
	2CMC PEO/Tween20	2.14	−3.23	1.65	0.99
	4CMC PEO/Tween20	3.12	−5.30	4.05	0.99
	0.5CMC PEO/SDS	2.77	−4.14	2.49	0.99
	1CMC PEO/SDS	2.34	−2.06	0.06	0.99
	2CMC PEO/SDS	2.40	−2.76	1.22	0.99
	4CMC PEO/SDS	2.76	−4.26	2.80	0.99

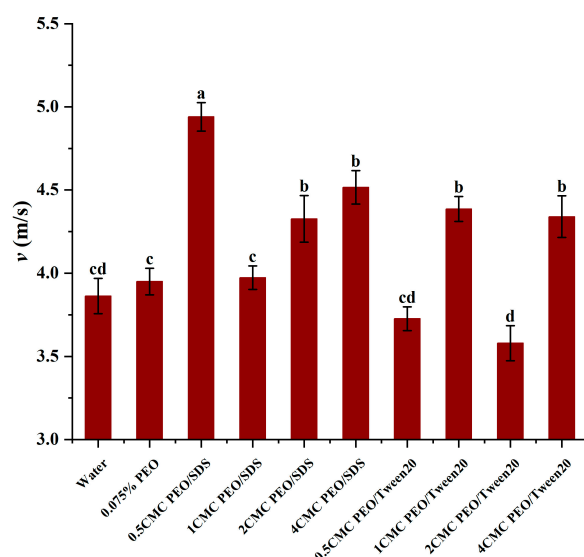


Figure 10. Droplet velocity distribution of different adjuvant combinations in the vertical direction below the spray nozzle. (Note: The graphs a,b,c,d are arranged according to the size of all means, with a representing the largest mean, and where there is a letter with the same labeling, the difference is not significant, and where there is a letter with a different labeling, the difference is significant.).

4. Discussion

In this study, a combination of high-molecular-weight polymer/surfactant adjuvants with concentrations and compositions similar to many agricultural adjuvants were used to measure the droplet size and velocity produced by different types and concentrations of high-molecular-weight polymer adjuvants based on the PDI measurement method. A sub-area statistical method was employed to statistically analyze the droplet characteristics at various points below the nozzle. The research conclusions are as follows.

(1) The aggregates formed by the combination of the conjugated surfactant and the polymer can reduce the equilibrium surface tension of the solution, and the equilibrium surface tension of the solution decreases gradually with the increase in the content of the associative surfactant. The viscosity of a polymer/associative surfactant increases with the increase in the concentration of associative surfactant. The addition of polymer/non-associative surfactant to the polymer did not show any significant change in the values of solution surface tension and viscosity.

(2) For polymer/associative surfactant combinations, the droplet size can be increased by increasing the amount of associative surfactant. For polymer/non-associative surfactant combinations, the droplet size formed by solution atomization decreases when a non-associative surfactant is added. The polymer/associative surfactant combination solution produces a larger spray angle during spray nozzle atomization. The uniformity in droplet size distribution of the polymer/non-associative surfactant combination solution is better than that of the polymer solution and the polymer/non-associative surfactant combination solution.

(3) At the same position, the droplet velocity of the atomized polymer/associative surfactant combination solution is enhanced compared with that of the aqueous solution. The pattern of droplet velocity formed by the atomization of the polymer/associative surfactant combination solution is not clear and needs to be further explored. The droplet velocities of different adjuvant combinations are fitted with a quadratic polynomial to the values on the x -axis, and the correlation coefficients are all above 0.9.

The binding of surfactants and PEO molecular chains causes dynamic extension, which is the main factor determining the spray performance. This study emphasizes the practicality of polymer/complex-forming surfactant systems in controlling solution atomization characteristics. Achieving optimal droplet size distributions by adding an

appropriate amount of complex-forming surfactant into high-molecular-weight polymer allows for the maximizing of pesticide efficacy and minimizing spray drift.

Author Contributions: Conceptualization, R.Z. and P.H.; methodology, P.H.; software, P.H.; validation, L.L., Q.T. and P.H.; formal analysis, P.H.; investigation, P.H. and R.Z.; resources, R.Z. and L.C.; data curation, P.H., W.Y. and J.Y.; writing—original draft preparation, P.H.; writing—review and editing, P.H., L.L. and R.Z.; visualization, P.H.; supervision, R.Z.; project administration, R.Z. and L.C.; funding acquisition, R.Z. and L.C. All authors have read and agreed to the published version of the manuscript.

Funding: This research was funded by the National Natural Science Foundation of China, grant number 32071907 and the National Natural Science Foundation of China, grant number 32301706.

Institutional Review Board Statement: Not applicable.

Data Availability Statement: Data are contained within the article.

Conflicts of Interest: The authors declare no conflicts of interest.

References

- Hu, P.; Zhang, R.; Yang, J.; Chen, L. Development Status and Key Technologies of Plant Protection UAVs in China: A Review. *Drones* **2022**, *6*, 354. [[CrossRef](#)]
- Kang, F.; Wu, X.; Wang, Y.; Zheng, Y.; Li, S.; Chen, C. Research progress and prospect of pesticide droplet deposition characteristics. *Trans. Chin. Soc. Agric. Eng. (Trans. CSAE)* **2021**, *37*, 1–14.
- Tuck, C.R.; Ellis, M.C.B.; Miller, P.C.H. Techniques for measurement of droplet size and velocity distributions in agricultural sprays. *Crop Prot.* **1997**, *16*, 619–628. [[CrossRef](#)]
- Zhang, H.; Zheng, J.; Zhou, H.; Dorr, G.J. Droplet deposition distribution and off-target drift during pesticide spraying operation. *Trans. Chin. Soc. Agric. Mach.* **2017**, *48*, 117–122.
- Xue, S.; Han, J.; Xi, X.; Lan, Z.; Wen, R.; Ma, X. Coordination of distinctive pesticide adjuvants and atomization nozzles on droplet spectrum evolution for spatial drift reduction. *Chin. J. Chem. Eng.* **2024**, *66*, 250–262. [[CrossRef](#)]
- Samples, C.A.; Butts, T.R.; Vieira, B.C.; Irby, J.T.; Reynolds, D.B.; Catchot, A.; Kruger, G.R.; Dodds, D.M. Effect of Deposition Aids Tank-Mixed with Herbicides on Cotton and Soybean Canopy Deposition and Spray Droplet Parameters. *Agronomy* **2021**, *11*, 278. [[CrossRef](#)]
- Zhang, S.; Huang, M.; Zhou, Q.; Jiao, Y.; Sun, H.; Cheng, X.; Xue, X. Study on Effects of Different Concentration Adjuvants on the Properties of Prochloraz Emulsion in Water Solution Droplets and Deposition. *Agronomy* **2023**, *13*, 2635. [[CrossRef](#)]
- Dorr, G.; Hanan, J.; Adkins, S.; Hewitt, A.; O'Donnell, C.; Noller, B. Spray deposition on plant surfaces: A modelling approach. *Funct. Plant Biol.* **2008**, *35*, 988–996. [[CrossRef](#)]
- Griesang, F.; Spadoni, A.B.D.; Ferreira, P.H.U.; Ferreira, M.D.C. Effect of working pressure and spacing of nozzles on the quality of spraying distribution. *Crop Prot.* **2022**, *151*, 105818. [[CrossRef](#)]
- Gu, C.; Zou, W.; Wang, X.; Chen, L.; Zhai, C. Wind loss model for the thick canopies of orchard trees based on accurate variable spraying. *Front. Plant Sci.* **2022**, *13*, 1010540. [[CrossRef](#)]
- Li, L.; Hu, Z.; Liu, Q.; Yi, T.; Han, P.; Zhang, R.; Pan, L. Effect of flight velocity on droplet deposition and drift of combined pesticides sprayed using an unmanned aerial vehicle sprayer in a peach orchard. *Front. Plant Sci.* **2022**, *13*, 981494. [[CrossRef](#)] [[PubMed](#)]
- Zhang, R.; Hewitt, A.J.; Chen, L.; Li, L.; Tang, Q. Challenges and opportunities of unmanned aerial vehicles as a new tool for crop pest control. *Pest. Manag. Sci.* **2023**, *79*, 4123–4131. [[CrossRef](#)] [[PubMed](#)]
- Zhang, R.; Zhang, Z.; Xu, G.; Chen, L.; Hewitt, A.J. Effect of spray adjuvant types and concentration on nozzle atomization. *Trans. Chin. Soc. Agric. Eng.* **2018**, *34*, 36–43.
- Li, X.; Chen, L.; Tang, Q.; Li, L.; Chen, W.; Hu, P.; Zhang, R. Characteristics on the Spatial Distribution of Droplet Size and Velocity with Difference Adjuvant in Nozzle Spraying. *Agronomy* **2022**, *12*, 1960. [[CrossRef](#)]
- Li, X.; Zhang, R.; Tang, Q.; Li, L.; Ding, C.; Chen, L. Experimental study on the spatial distribution of spray nozzle atomization droplet size and velocity. *J. Agric. Mech. Res.* **2024**, *46*, 159–167.
- Zhang, J.; Song, J.; He, X.; Zeng, A.; Liu, Y. Droplets movement characteristics in atomisation process of flat fan nozzle. *Trans. Chin. Soc. Agric. Mach.* **2011**, *42*, 66–69, 75.
- Li, S.; Chen, C.; Wang, Y.; Kang, F.; Li, W. Study on the Atomization Characteristics of Flat Fan Nozzles for Pesticide Application at Low Pressures. *Agriculture* **2021**, *11*, 309. [[CrossRef](#)]
- Chen, C.; Li, S.; Wu, X.; Wang, Y.; Kang, F. Analysis of droplet size uniformity and selection of spray parameters based on the biological optimum particle size theory. *Environ. Res.* **2022**, *204*, 112076. [[CrossRef](#)]
- Vallet, A.; Tinet, C. Characteristics of droplets from single and twin jet air induction nozzles: A preliminary investigation. *Crop Prot.* **2013**, *48*, 63–68. [[CrossRef](#)]

20. Thompson, J.C.; Rothstein, J.P. The atomization of viscoelastic fluids in flat-fan and hollow-cone spray nozzles. *J. Non-Newton. Fluid Mech.* **2007**, *147*, 11–22. [[CrossRef](#)]
21. Roudini, M.; Wozniak, G. Experimental investigation of spray characteristics of pre-filming air-blast atomizers II—Influence of liquid properties. *J. Appl. Fluid Mech.* **2019**, *13*, 679–691. [[CrossRef](#)]
22. Tang, Q.; Zhang, R.; Chen, L.; Deng, W.; Xu, M.; Xu, G.; Li, L.; Hewitt, A. Numerical simulation of the downwash flow field and droplet movement from an unmanned helicopter for crop spraying. *Comput. Electron. Agric.* **2020**, *174*, 105468. [[CrossRef](#)]
23. Zheng, Z.; Xue, X.; Song, S.; Li, Z.; Dai, Q.; Li, K.; Xu, X. Investigation of nozzle spray pressure and droplet particle size and velocity distribution based on hollow conical fog single nozzle. *J. Agric. Mech. Res.* **2021**, *43*, 110–117.
24. Ruobing, W.; Gary, D.; Hewitt, A.; Cooper-White, J. Impacts of polymer/surfactant interactions on spray drift. *Colloids Surf. A Physicochem. Eng. Asp.* **2016**, *500*, 88–97.
25. Li, C.; He, R.; He, Z.; Kumar, S.S.; Fredericks, S.A.; Hogan, C.J.; Hong, J. Spatially-resolved characterization of oil-in-water emulsion sprays. *Int. J. Multiph. Flow* **2021**, *145*, 103813. [[CrossRef](#)]
26. Cao, J. *Liquid Atomization*; Peking University Press: Beijing, China, 2013.
27. Sun, S.; Tang, Y.; Miao, A.; Hou, C.; Zhuang, J.; Lin, T.; Luo, S. Research on atomization performance of fan and hollow cone nozzle of plant protection drone. *Jiangsu Agric. Sci.* **2019**, *47*, 246–250.
28. Smitter, L.M.; Guédez, J.F.; Müller, A.J.; Sáez, A.E. Interactions between Poly (ethylene Oxide) and Sodium Dodecyl Sulfate in Elongational Flows. *J. Colloid Interface Sci.* **2001**, *236*, 343–353. [[CrossRef](#)]
29. Tsuji, Y.; Morikawa, Y. LDV measurements of an air-solid two-phase flow in a horizontal pipe. *J. Fluid Mech.* **1982**, *120*, 385–409. [[CrossRef](#)]
30. Erik, M.; Justin, C.W. The effects of chain conformation in the microfluidic entry flow of polymer–surfactant systems. *J. Non-Newton. Fluid Mech.* **2009**, *160*, 22–30.
31. Iaroslav, M.; Elizabeth, R.A.; Steven, A.F.; Christine, M.C.; Cari, S.D. A review of liquid sheet breakup: Perspectives from agricultural sprays. *J. Aerosol Sci.* **2021**, *157*, 105805.
32. Antoine, G.; Rick, S.; Daniel, B. What determines the drop size in sprays of polymer solutions? *J. Non-Newton. Fluid Mech.* **2022**, *305*, 104813.
33. Cabane, D.R.B. Organization of surfactant micelles adsorbed on a polymer molecule in water: A neutron scattering study. *J. Phys. Fr.* **1982**, *43*, 1529–1542. [[CrossRef](#)]
34. Nikas, Y.J.; Blankshtein, D. Complexation of nonionic polymers and surfactants in dilute aqueous solutions. *Langmuir* **1994**, *10*, 3512–3528. [[CrossRef](#)]
35. Goddard, E.D. Polymer-surfactant interaction Part I. uncharged water-soluble polymers and charged surfactants. *Colloids Surf.* **1986**, *19*, 255–300. [[CrossRef](#)]
36. *ASAE Standards S572; Spray Nozzle Classification by Droplet Spectra*. ASAE: St. Joseph, MI, USA, 2004.

Disclaimer/Publisher’s Note: The statements, opinions and data contained in all publications are solely those of the individual author(s) and contributor(s) and not of MDPI and/or the editor(s). MDPI and/or the editor(s) disclaim responsibility for any injury to people or property resulting from any ideas, methods, instructions or products referred to in the content.